PROCEEDINGS OF SPIE

SPIEDigitalLibrary.org/conference-proceedings-of-spie

Development of a real-time solver for the local eigenvalue modification procedure

Ogunniyi, Emmanuel, Downey, Austin R., Bakos, Jason

Emmanuel A. Ogunniyi, Austin R. J. Downey Jr., Jason D. Bakos, "Development of a real-time solver for the local eigenvalue modification procedure," Proc. SPIE 12046, Sensors and Smart Structures Technologies for Civil, Mechanical, and Aerospace Systems 2022, 120460U (18 April 2022); doi: 10.1117/12.2613208

Event: SPIE Smart Structures + Nondestructive Evaluation, 2022, Long Beach, California, United States

SPIE.

Downloaded From: https://www.spiedigitallibrary.org/conference-proceedings-of-spie on 19 Apr 2022 Terms of Use: https://www.spiedigitallibrary.org/terms-of-use

Development of Real-time Solver for Local Eigenvalue Modification Procedure

Emmanuel A. Ogunniyi[a], Austin R.J. Downey[a,b], and Jason D. Bakos[c]

[a]Department of Mechanical Engineering, University of South Carolina, Columbia, USA
[b]Department of Civil and Environmental Engineering, University of South Carolina, Columbia, USA
[c]Department of Computer Science & Engineering, University of South Carolina, Columbia, USA

ABSTRACT

Real-time model updating for active structures experiencing high-rate dynamic events such as; hypersonic vehicles, active blast mitigation, and ballistic packages require that continuous changes in the structure's state be updated on a timescale of 1 ms or less. This requires the development of real-time model updating techniques capable of tracking the structure's state. The Local Eigenvalue Modification Procedure (LEMP) is a structural dynamic modification procedure that converts the computationally intensive global eigenvalue problem used in modal analysis into a set of second-order equations that are more readily handled. Implementation of LEMP for tracking a structure's state results in secular equations that must be solved to obtain the modified eigenvalues of the structure's state. In this work, the roots of the secular equations are solved iteratively using a divide and conquer approach, leading to faster root convergence. The present study reports on developing a real-time computing module to perform LEMP in the context of real-time model updating with a stringent timing constraint of 1 ms or less. In this preliminary work, LEMP is applied to tracking the condition of a numerical cantilever beam structure, which depicts changes in a structure's state as a change in the roller position. A discussion of variations in timing results and accuracy are discussed.

Keywords: real-time model updating, high-rate dynamics, eigenvalue modification, state estimation

1. INTRODUCTION

Real-time updating of structures experiencing high-rate dynamics is significant in predicting the behavior of the structures. High-rate dynamics systems such as hypersonic vehicles, impact protection systems, ballistic, and active blast mitigation systems operate at timescales of less than 100 ms with a high amplitude of over 100 g_n. These high-rate dynamic structures are characterized by large uncertainty in external loads, high levels of non-stationarity, severe disruptions, and the formation of unmodeled dynamics from changes in system events.[1] The ability to measure, estimate, and predict these structures' varying states overtime is beneficial for the development of next-generation control systems.[2] One way to track the state of structures operating in high-rate dynamic environments is to use structural model updating to update the system state in real-time.[3,4] A system that can track the state of a structure undergoing high-rate dynamic events must have a model updating technique that is flexible in order to adapt and learn changing external load conditions without relying on pre-trained data. The system must also be capable of updating within a 1 ms timescale to allow real-time data-driven decisions to be made online.[2]

For civil and aeronautical structures, real-time model updating approaches have been established, primarily using Finite Element Analysis (FEA).[5–8] However, due to the computing expenses associated with solving FEA models, the execution time requirements in these initiatives were from hours to months, and they were frequently

Further author information: (Send correspondence to Emmanuel A. Ogunniyi)
Emmanuel A. Ogunniyi: Email: ogunniyi@email.sc.edu
Austin R.J. Downey: Email: austindowney@sc.edu
Jason D. Bakos: Email: jbakos@cse.sc.edu

Sensors and Smart Structures Technologies for Civil, Mechanical, and Aerospace Systems 2022, edited by Daniele Zonta, Branko Glisic, Zhongqing Su, Proc. of SPIE Vol. 12046, 120460U · © 2022 SPIE · 0277-786X · doi: 10.1117/12.2613208

Downloaded From: https://www.spiedigitallibrary.org/conference-proceedings-of-spie on 19 Apr 2022
Terms of Use: https://www.spiedigitallibrary.org/terms-of-use

done offline. Furthermore, the implementation of a finite element analysis with pre-calculated databases of structural conditions for this type of structure is limited due to the system's unmodeled dynamics, which are common in high-rate dynamic events.[1] Resolving the difficulty of accounting for unmodeled dynamics involves the development of online model updating systems that can track the system's state with minimal offline training.

The authors previously showed that by utilizing a simplified Euler-Bernoulli beam model and updating the model in the frequency domain, real-time model updating could be achieved for a structure undergoing a simulated high-rate event with a latency limit of 1 ms.[4] However, the FEA model had to be reduced to 23 nodes to achieve the 1 ms constraint. The generalized eigenvalue problem took 0.6 ms to solve in this arrangement, accounting for most of the computational load. Furthermore, due to its $O(n^3)$ complexity, the generalized eigenvalue formulation scales poorly for larger FEA models.

In this paper, real-time modeling is performed utilizing the local eigenvalue modification process (LEMP) to simplify state equations on an Euler-Bernoulli beam of five nodes undergoing a single-state change.[9,10] All variables for the altered state are specified in terms of the initial state and changes made between the current and initial state. Only information for the degrees of freedom (DOF) at which changes occur is required when using LEMP. Since the solutions to the initial state equations are constant, this decreases the number of calculations required. Furthermore, LEMP reduces the initial eigenvalue solution to a collection of second-order equations that can be easily solved. The resulting set of secular equations of complexity $O(n^2)$ as compared to the general eigenvalue problem of complexity $O(n^3)$ is then solved using the divide and conquer approach. Li Ren-Cang developed an efficient approach to solve the secular equation using divide and conquer which takes less than four iterations to arrive at the expected root of the equation.[11] The divide and conquer approach solves for each root sequentially; hence, reducing computational requirements. The divide and conquer algorithm is less complex than other functions for solving the roots of equations.

The contributions of this work are 1) Introduction of the divide and conquer approach in the LEMP algorithm to solve the resulting secular equation, leading to faster root convergence, and; 2). Validation of the LEMP algorithm accuracy using a simple Euler-Bernoulli beam against the full-rank generalized eigenvalue approach. Also, algorithm timing, complexity, and error induced by the replacement of the Sympy function "solveset" with the divide and conquer approach in the LEMP algorithm are investigated and discussed.

2. BACKGROUND STUDIES

This section provides background information on solving the generalized eigenvalue problem in addition to the use of LEMP for solving a single state change for a system.

2.1 Generalized Eigenvalue

Neglecting damping effects, the equation of motion for a system's initial state, can be found in Eq. 1 below.

$$\mathbf{M}_1\ddot{x} + \mathbf{K}_1 x = 0 \tag{1}$$

$\ddot{x}$ and x represent the acceleration and displacement in physical space, respectively. Moreover, $\mathbf{M}_1$ and $\mathbf{K}_1$ are the system's mass and stiffness matrices in physical space where the subscript 1 represents that they are in their initial state. Both matrices are square symmetric and have dimensions of $n \times n$, with n being the system's degree of freedom.The generalized eigenvalue problem for Eq. 1 is defined as $\mathbf{K}_1\mathbf{U}_1 = \mathbf{M}_1\mathbf{U}_1\boldsymbol{\lambda}$, Eq. 2 and Eq. 3 below can be used to solve the GE problem.

$$\det[\mathbf{K}_1 - \boldsymbol{\lambda}\mathbf{M}_1] = 0 \tag{2}$$

$$[\mathbf{K}_1 - \boldsymbol{\lambda}\mathbf{M}_1]\mathbf{U}_1 = 0 \tag{3}$$

The eigenvalues $\boldsymbol{\lambda}$ and eigenvectors $\mathbf{U}_1$ are shown in Eq. 4 and Eq. 5, which are the squares of the first n natural frequencies and the first n modal vectors for the system respectively. It is important to note that the modal matrix in eq 5 is not the same as mode shapes, although it can be used to calculate them.

$$\boldsymbol{\lambda} = \begin{bmatrix} \omega_1^2 & 0 & 0 & 0 \\ 0 & \omega_2^2 & 0 & 0 \\ 0 & 0 & \ddots & 0 \\ 0 & 0 & 0 & \omega_n^2 \end{bmatrix} \tag{4}$$

Downloaded From: https://www.spiedigitallibrary.org/conference-proceedings-of-spie on 19 Apr 2022
Terms of Use: https://www.spiedigitallibrary.org/terms-of-use

$$\mathbf{U}_1 = \begin{bmatrix} \vec{u}_1^1 & \vec{u}_2^1 & \cdots & \vec{u}_n^1 \end{bmatrix} \tag{5}$$

2.2 Local Eigenvalue Modification Procedure

By monitoring changes in the system's dynamic response, such as frequencies and mode shapes, structural dynamic modification (SDM) identifies physical alterations made to the system parameters such as mass, stiffness, or damping.[12–14] SDM is performed by using mass, stiffness, or damping matrices to model the altered state as a mixture of the initial state and the changes made to the initial state in the EOM for the altered system. SDM employs the modal synthesis principle, which states that any dynamic response of a vibrating structure can be decomposed into a set of individual contributions of single frequencies,[15,16] effectively defining the initial system of n DOF as a collection of n independent single DOF systems. Each independent DOF corresponds to one natural frequency of the modal system with a modal mass and stiffness value which are related to the physical system response through modal transformation. The changes made to the initial system results in an altered modal system.

Weissenburger created LEMP in 1968 to avoid eigenvalue solutions in SDM when just one change is made to the system. The goal was to make state calculations easier because computers at the time had limited processing capability.[9,17,18] To do this, LEMP uses a single GE solution for the initial system and simplifies altered state equations by translating them into modal space, isolating the DOFs that contribute to state changes, and formulating equations in terms of the initial state, as explained in SDM. However, additional simplifications are achieved by truncating the n independent single degree of systems to include the m modes of interest. This yields a matrix with dimensions of $m \times m$ and a modal matrix $\mathbf{U}_1$ with dimensions of $n \times m$.

This modal reduction further simplifies the altered state equations. Figure 1 depicts an overview of the LEMP algorithm, which will be expanded upon using a numerical system later in this work. The GE equation is reduced to a set of second-order equations whose roots are determined by the system's initial frequencies, resulting in a smaller domain over which the problem can be solved.[9] These simplifications lower the number and complexity of equations required to compute the structure's state, leading to shorter computation times.

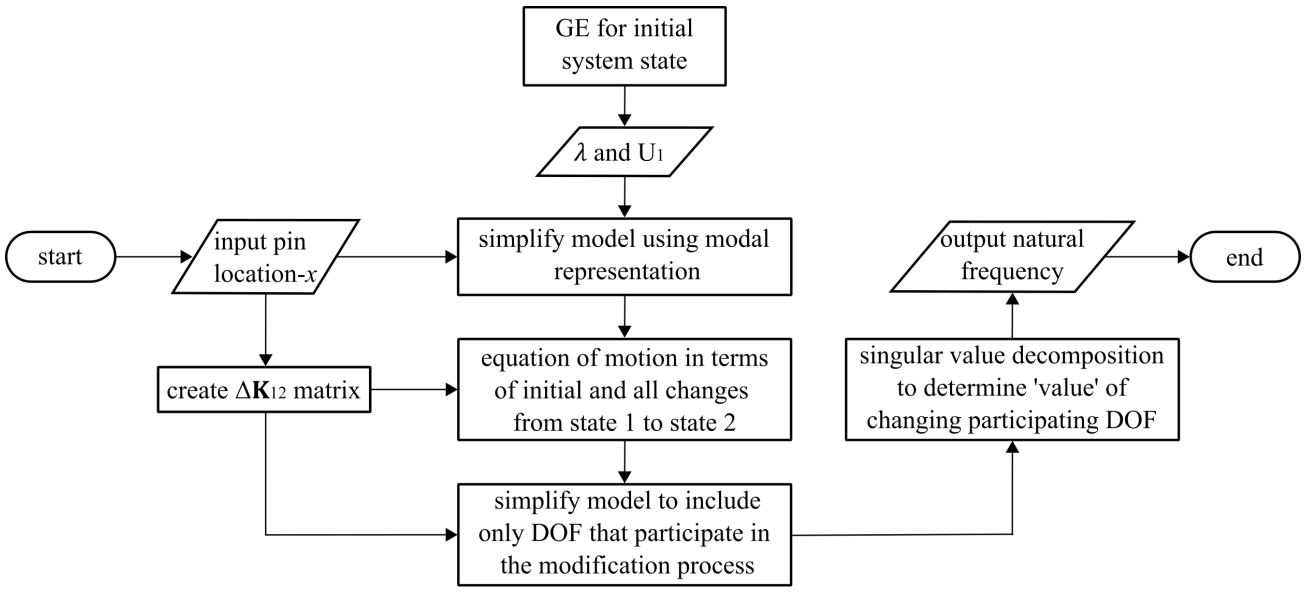
GE for initial system state
λ and U1
start
input pin location-x
simplify model using modal representation
output natural frequency
end
create ΔK12 matrix
equation of motion in terms of initial and all changes from state 1 to state 2
singular value decomposition to determine 'value' of changing participating DOF
simplify model to include only DOF that participate in the modification process

Figure 1: Flowchart detailing the for making a single-state change to a structural system.

Downloaded From: https://www.spiedigitallibrary.org/conference-proceedings-of-spie on 19 Apr 2022
Terms of Use: https://www.spiedigitallibrary.org/terms-of-use

3. METHODOLOGY

3.1 LEMP Process Algorithm

The technique for applying LEMP is depicted in Figure 1. After obtaining the GE solution for the initial state, the EOM for the altered state will be built using Eq. 6 while ignoring the damping effects.[10]

$$\mathbf{M}_2\ddot{x} + \mathbf{K}_2 x = 0 \tag{6}$$

$\mathbf{M}_2$ and $\mathbf{K}_2$ are the altered state's mass and stiffness matrices in physical space, both with dimensions of $n \times n$. The addition of a roller boundary condition at a node along the beam results in a change in the system state. This restricts bending in the beam at that position with FEA, leading to row and column cancellation. There is only change to the stiffness matrix, which is indicated by $\Delta\mathbf{K}_{12}$ and has dimensions of $n \times n$. As illustrated in Eq. 7, mass and stiffness of the altered state are defined in terms of the initial state and variations between the two.

$$\mathbf{M}_2 = \mathbf{M}_1, \qquad \mathbf{K}_2 = \mathbf{K}_1 + \Delta\mathbf{K}_{12} \tag{7}$$

Eq. 8 is obtained by substituting Eq. 7 into the initial EOM for the altered state.

$$\mathbf{M}_1\ddot{x} + \big(\mathbf{K}_1 + \Delta\mathbf{K}_{12}\big)x = 0 \tag{8}$$

The m modes of the initial state's n independent single DOF systems are reduced to only include the m modes of interest to ease calculations. This yields a matrix with $m \times m$ dimensions and a corresponding modal matrix $\mathbf{U}_1$ with $n \times m$ dimensions. The system response is transformed from physical to modal space using Eq. 9, where q_1 and $\ddot{q}_1$ are the system displacement and acceleration vectors in modal space, respectively.

$$x = \mathbf{U}_1 q_1, \qquad \ddot{x} = \mathbf{U}_1\ddot{q}_1 \tag{9}$$

Eq. 10 is obtained by converting the EOM to modal space using Eq. 9.

$$\mathbf{M}_1\mathbf{U}_1\ddot{q}_1 + \big(\mathbf{K}_1 + \Delta\mathbf{K}_{12}\big)\mathbf{U}_1 q_1 = 0 \tag{10}$$

The mass and stiffness matrices are normalized in modal space by multiplying each term by $\mathbf{U}_1^{\mathrm{T}}$, yielding diagonal matrices shown in Eq. 11.

$$\mathrm{diag}(\overline{\mathbf{M}}_1)\ddot{q}_1 + \big[\mathrm{diag}(\overline{\mathbf{K}}_1) + \Delta\overline{\mathbf{K}}_{12}\big]q_1 = 0 \tag{11}$$

$\overline{\mathbf{M}}_1$ and $\overline{\mathbf{K}}_1$ are the modal mass and stiffness matrices, respectively, and $\Delta\overline{\mathbf{K}}_{12}$ is the difference in modal space between the initial and altered states. After modal truncation, these matrix dimensions are reduced from $n \times n$ to $m \times m$. Eq. 12 is obtained by scaling Eq. 11 to unit modal mass, where $\mathbf{I}$ is the identity matrix with dimensions of $m \times m$.

$$\mathbf{I}\ddot{q}_1 + \big[\boldsymbol{\lambda} + \Delta\overline{\mathbf{K}}_{12}\big]q_1 = 0 \tag{12}$$

The following approach is used to solve for the updated natural frequencies that occur as a result of system changes. The GE solution of Eq. 12 is first obtained, but not solved, as shown in Eq. 13.

$$\det\big[(\boldsymbol{\lambda} + \Delta\overline{\mathbf{K}}_{12}) - \boldsymbol{\Lambda}\mathbf{I}\big] = 0, \qquad \big[(\boldsymbol{\lambda} + \Delta\overline{\mathbf{K}}_{12}) - \boldsymbol{\Lambda}\mathbf{I}\big]q_{12} = 0 \tag{13}$$

$\boldsymbol{\Lambda}$ is a $m \times m$-dimensional matrix with the squares of the updated frequencies as diagonals and q_{12} as the modal change between states. Eq. 14 is then obtained by rearranging the terms.

$$\big[(\boldsymbol{\lambda} - \boldsymbol{\Lambda}) + \Delta\overline{\mathbf{K}}_{12}\big]q_{12} = 0 \tag{14}$$

Downloaded From: https://www.spiedigitallibrary.org/conference-proceedings-of-spie on 19 Apr 2022
Terms of Use: https://www.spiedigitallibrary.org/terms-of-use

Due to the applied nodal boundary condition, stiffness change occurs between the state, hence only the diagonal values of the $\mathbf{K}_1$ and $\mathbf{K}_2$ matrices will be changed. Furthermore, the diagonal value associated with the DOF where the roller is placed is the only non-zero term in the $\Delta\mathbf{K}_{12}$ matrix. The equation for $\Delta\mathbf{K}_{12}$ is then simplified to contain information from the contributing nodes, noting that the only non-zero values in $\Delta\overline{\mathbf{K}}_{12}$ are those connected with the DOF(s) that undergo a change in stiffness from the initial to a changed state. Eq. 15 is used for spectral decomposition of $\Delta\mathbf{K}_{12}$.

$$\Delta\overline{\mathbf{K}}_{12} = \mathbf{T}\text{diag}(\boldsymbol{\alpha})\mathbf{T}^{\mathrm{T}} \tag{15}$$

$\mathbf{T}$, Eq. 16 is a tie matrix, $\mathbf{T}$ is a vector with an over-right arrow to denote it as a vector and $\boldsymbol{\alpha}$ is a $m \times m$ matrix. Eq. 17 shows how to convert Eq. 15 to modal space.

$$\mathbf{T} = \begin{bmatrix} \vec{t}_1 & \vec{t}_2 & \cdots & \vec{t}_n \end{bmatrix} \tag{16}$$

$$\Delta\overline{\mathbf{K}}_{12} = \mathbf{U}_1^{\mathrm{T}}\mathbf{T}\text{diag}(\boldsymbol{\alpha})\mathbf{T}^{\mathrm{T}}\mathbf{U}_1 \tag{17}$$

By reducing $\Delta\overline{\mathbf{K}}_{12}$ to just contain non-zero values denoted by $\Delta\mathbf{k}_{12}$, the contributing values of $\Delta\overline{\mathbf{K}}_{12}$ can be redefined. The tie vector and alpha value of the affected DOF, represented by t_c and α respectively, are used to do this. These reduced matrices are constructed using the relation in Eq. 18 where v is the one-dimensional contribution vector.

$$\vec{v} = \mathbf{U}_{1_c}^{\mathrm{T}}\vec{t}_c, \qquad \vec{v} = \begin{bmatrix} v_1 & v_2 & \cdots & v_m \end{bmatrix} \tag{18}$$

To solve for $\Delta\overline{\mathbf{k}}_{12}$, Eq. 18 is combined with the alpha value associated with the affected DOF as shown in Eq. 19, which gives the modal stiffness change equation for contributing nodes.

$$\Delta\overline{\mathbf{k}}_{12} = \vec{v}\alpha\vec{v}^{\mathrm{T}} \tag{19}$$

Since $\Delta\overline{\mathbf{k}}_{12}$ is the same as $\Delta\overline{\mathbf{K}}_{12}$, Eq. 19 can be substituted for $\Delta\overline{\mathbf{K}}_{12}$ in the initial GE shown in Eq. 13, yielding the following equations:

$$\left[(\boldsymbol{\lambda} - \boldsymbol{\Lambda}) + \vec{v}\alpha\vec{v}^{\mathrm{T}}\right]q_{12} = 0, \qquad (\boldsymbol{\lambda} - \boldsymbol{\Lambda})q_{12} + \vec{v}\alpha\vec{v}^{\mathrm{T}}q_{12} = 0 \tag{20}$$

$\mathbf{S}$ is defined as an arbitrary variable in Eq. 21 to further simplify the state equations.

$$\mathbf{S} = \vec{v}^{\mathrm{T}}q_{12} \tag{21}$$

The result is Eq. 22, which is obtained by substituting Eq. 21 into Eq. 20.

$$(\boldsymbol{\lambda} - \boldsymbol{\Lambda})q_{12} + \vec{v}\alpha\mathbf{S} = 0 \tag{22}$$

Eq. 22 can be rearranged to solve for q_{12}, as demonstrated in Eq. 23. Eq. 23 is then multiplied by $\vec{v}^{\mathrm{T}}$ to give Eq. 24.

$$q_{12} = -(\boldsymbol{\lambda} - \boldsymbol{\Lambda})^{-1}\vec{v}\alpha\mathbf{S} \tag{23}$$

$$\vec{v}^{\mathrm{T}}q_{12} = -\vec{v}^{\mathrm{T}}(\boldsymbol{\lambda} - \boldsymbol{\Lambda})^{-1}\vec{v}\alpha\mathbf{S} \tag{24}$$

Using the relation from Eq. 21, this may be expressed as Eq. 25.

$$\mathbf{S} = -\vec{v}^{\mathrm{T}}(\boldsymbol{\lambda} - \boldsymbol{\Lambda})^{-1}\vec{v}\alpha\mathbf{S} \tag{25}$$

Downloaded From: https://www.spiedigitallibrary.org/conference-proceedings-of-spie on 19 Apr 2022
Terms of Use: https://www.spiedigitallibrary.org/terms-of-use

Both $\mathbf{S}$ matrices are eliminated by multiplying each side by $\mathbf{S}^{-1}$, leaving the matrix equation presented in Eq. 26.

$$\alpha^{-1} = -\vec{v}^{\mathrm{T}}(\boldsymbol{\lambda} - \boldsymbol{\Lambda})^{-1}\vec{v} \tag{26}$$

$\vec{v}$ is element-wise equal to $\vec{v}^{\mathrm{T}}$ because it is a one-dimensional vector. As a result, decomposing Eq. 26 into its constituents components produces Eq. 27, with the sole unknown being Ω_r^2, or the natural frequency of the altered state. The number of modes used to characterize the system is m, and r ranges from 1 to m.

$$\frac{-1}{\alpha} = \sum_{r=1}^{m} \frac{v_r^2}{\omega_r^2 - \Omega_r^2} \tag{27}$$

In summary, LEMP is made up of a single general eigenvalue solution for the system's initial state and an eigenvalue modification process that is updated for each change in the state. The eigenvalue modification method simplifies state equations by characterizing the system in terms of the initial state and modifications made to the altered state.

3.2 Solving the secular equation

The secular equation is defined as

$$0 = \frac{1}{\alpha} + \sum_{k=1}^{m} \frac{v_k^2}{\omega_k^2 - x} \tag{28}$$

Eq. 28 has m possible values of x that will be obtained using the divide and conquer approach. The divide and conquer approach solves for each eigenvalue separately. It start by selecting an initial guess (y) for the first eigenvalue[11] where y is the starting value for x . The selected value lies between ω_k and ω_{k+1}. To make a correct decision, the sign of $f(\frac{\omega_k+\omega_{k+1}}{2})$ must be checked, if positive, λ_k lies closer to ω_k than to ω_{k+1}.

First, consider the case where $1 \leq k < n$. The secular function Eq. 28 is rewritten as Eq. 29.

$$g(x) = \frac{1}{\alpha} + \sum_{r=1, r\neq k,k+1}^{m} \frac{v_r^2}{\omega_r^2 - x}, \quad \text{and} \quad h(x) = \frac{v_k^2}{\omega_k^2 - x} + \frac{v_{k+1}^2}{\omega_{k+1}^2 - x} \tag{29}$$

Then choose the right initial guess y from the two root of Eq. 30

$$g\Big(\frac{\omega_k + \omega_{k+1}}{2}\Big) + h(y) = 0 \tag{30}$$

In the case where $\frac{\omega_k+\omega_{k+1}}{2} \geq 0$, solve for $\tau = y - \omega_k$, else solve for $\tau = y - \omega_{k+1}$.

Define $\boldsymbol{\Delta} = \omega_{k+1} - \omega_k$ and $c = g\big(\frac{\omega_k+\omega_{k+1}}{2}\big)$

$$\tau = y - \omega_k = \frac{a - \sqrt{a^2 - 4bc}}{2c} \quad if \;\; a \leq 0 \tag{31}$$

$$= \frac{2b}{a + \sqrt{a^2 - 4bc}} \quad if \;\; a > 0 \tag{32}$$

where if $f\big(\frac{\omega_k+\omega_{k+1}}{2}\big) \geq 0$,

$$K = k, a = c\boldsymbol{\Delta} + \big(v_k^2 + v_{k+1}^2\big), \quad b = v_k^2\boldsymbol{\Delta} \tag{33}$$

Downloaded From: https://www.spiedigitallibrary.org/conference-proceedings-of-spie on 19 Apr 2022
Terms of Use: https://www.spiedigitallibrary.org/terms-of-use

where if $f\big(\frac{\omega_k+\omega_{k+1}}{2}\big) < 0$,

$$K = k+1, a = -c\boldsymbol{\Delta} + \left(v_k^2 + v_{k+1}^2\right), \quad b = -v_{k+1}^2\boldsymbol{\Delta} \tag{34}$$

After obtaining the initial guess for y, compute a correction η to y for a "better" next approximation $y+\eta$ to λ_k using Eq. 35 and Eq. 36.

$$\boldsymbol{\Delta}_k = \omega_k - y, \quad \boldsymbol{\Delta}_{k+1} = \omega_{k+1} - y, \quad x = y + \eta \tag{35}$$

$$\begin{aligned} a = (\boldsymbol{\Delta}_k + \boldsymbol{\Delta}_{k+1})f(y) - \boldsymbol{\Delta}_k\boldsymbol{\Delta}_{k+1}f^{'}(y), \quad b = \boldsymbol{\Delta}_k\boldsymbol{\Delta}_{k+1}f(y) \\ c = f(y) - \boldsymbol{\Delta}_k\psi_k^{'}(y) - \boldsymbol{\Delta}_{k+1}\phi_k^{'}(y) \\ = f(y) - \boldsymbol{\Delta}_{k+1}f^{'}(y) - \psi_k^{'}(y)(v_k^2 + v_{k+1}^2) \\ = f(y) - \boldsymbol{\Delta}_k f^{'}(y) - \phi_k^{'}(y)(v_k^2 + v_{k+1}^2) \end{aligned} \tag{36}$$

where $\psi_k(x)$ and $\phi_k(x)$ are obtained using Eq. 37

$$\psi_k(x) = \sum_{r=1}^{k}\frac{v_r^2}{\omega_r^2 - x}, \quad \phi_k(x) = \sum_{r=k+1}^{m}\frac{v_r^2}{\omega_r^2 - x} \tag{37}$$

$$\begin{aligned} \eta &= \frac{a - \sqrt{a^2 - 4bc}}{2c} \quad if\ a \le 0, \\ &= \frac{2b}{a + \sqrt{a^2 - 4bc}} \quad if\ a > 0 \end{aligned} \tag{38}$$

For case where $k = m$, obtain ω_{k+1} using Eq. 39,

$$\omega_{k+1} = \omega_k + \frac{v^{\mathrm{T}}v}{\rho} \tag{39}$$

After obtaining ω_{k+1}, repeat the rest of the steps same as when $k <$ mode. Iteration stopping criteria is given as,

$$\eta^2 \le \epsilon_m \ \min|\omega_k - x|, |\omega_{k+1} - x|(|\eta_0| - |\eta|) \tag{40}$$

The steps of the LEMP algorithm used for the state estimation through this paper are presented as Pseudocode in Algorithm 1.

Table 1 shows the major operations in the LEMP algorithm and their complexity level. These operations are those employed by the divide and conquer approach to solve for the altered state frequencies. Other operations in the LEMP algorithm are of $O(n)$ complexity, however, the divide and conquer approach is of complexity $O(n^2)$, hence, resulting in an overall LEMP algorithm complexity of $O(n^2)$.

Table 1: Major operations in the LEMP algorithm and their complexity.

Outermost loop	Innermost loop	Operation	Lines in Alg.	Complexity subtotal
i= 1: mode	k (< or = mode)	solve for a, b, c and τ	9, 14	$\xi_1 = O(n^2)$
i= 1: mode	k (< or = mode)	solve for initial value of y	10, 15	$\xi_2 = O(n)$
$i = 1$	k = mode	solve for ω_{k+1} required for k = mode	13	$\xi_3 = O(n^2)$

Downloaded From: https://www.spiedigitallibrary.org/conference-proceedings-of-spie on 19 Apr 2022
Terms of Use: https://www.spiedigitallibrary.org/terms-of-use

Algorithm 1 Pseudocode for the LEMP algorithm.

```
 1: procedure LEMP
 2:     Define spring node ($n$)
 3:     Build $\Delta\mathbf{K}$ matrix
 4:     Spectral decomposition of $\Delta\mathbf{K} \rightarrow$ T & $\alpha$
 5:     Set truncation to contributing nodes : $\vec{v} \leftarrow \vec{v}$ [0:mode],   $\omega_r^2 \leftarrow \omega_r^2$ [0:mode]
 6:     Solve the secular equation to obtain $\Omega_k^2$
 7:     for i in range (mode) do
 8:         if k < mode then
 9:             solve for a, b, c and $\tau$ using Eqs. 31, 32, 33 and 34
10:             $y \leftarrow \tau + \omega_k$
11:             Compute correction $\eta$ to y to obtain $\lambda_k$
12:         else if k = mode then
13:             $\omega_{k+1} \leftarrow \omega_k + \frac{\vec{v}^T\vec{v}}{\rho}$
14:             solve for a, b, c and $\tau$ using Eqs. 31, 32, 33 and 34
15:             $y \leftarrow \tau + \omega_k$
16:             Compute correction $\eta$ to y to obtain $\lambda_k$
17:         end if
18:     end for
19:     solve for the altered state frequency
20: end procedure
```

To determine the viability of LEMP, the estimated states using the GE and LEMP are compared using mean absolute error (MAE) and signal to noise ratio where the GE is the measured value, and the LEMP is the estimated value. The MAE value measures the numerical error between the GE and LEMP estimated states.[19,20] Eq. 41 and Eq. 42 show the formula for MAE and SNR, respectively.

$$\text{MEA} = \frac{\sum_{i=1}^{z} |x_{\text{true}_i} - x_{\text{est}_i}|}{z} \tag{41}$$

$$\text{SNR}_{\text{dB}} = 10\,\log_{10}\left(\frac{P_{\text{signal}}}{P_{\text{noise}}}\right) \tag{42}$$

4. RESULTS AND DISCUSSION

4.1 Single-state change updating with LEMP

To estimate the state change, a beam of 5 nodes which corresponds to 10 DOF for Euler-Bernoulli beam ($n = 10$) as shown in figure 2 with properties shown in table 2 was used. Only the first five modes to determine state changes to the system (beam).

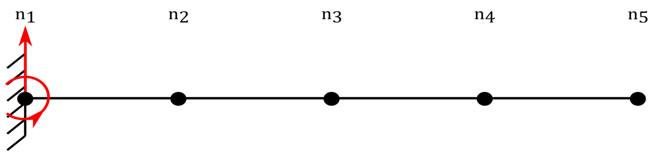

Figure 2: Initial state of the system (beam).

Downloaded From: https://www.spiedigitallibrary.org/conference-proceedings-of-spie on 19 Apr 2022
Terms of Use: https://www.spiedigitallibrary.org/terms-of-use

Table 2: Properties of the beam used in state-estimation process.

Properties	value
Density - ρ (kg/m^3)	7900
Cross-sectional area - $\mathrm{A_c}$ (m^2)	0.000306
Total length - l (m)	0.35
Elemental length - l_i (m)	0.35
Young's Modulus - E (Pa)	2e11

Construct the elemental mass and stiffness matrices (**M1** and **K1**) which are Eq. 43 and Eq. 44 written in the appendix of this paper using the Euler-Bernoulli formular. Then solve the general eigenvalue problem to obtain the squares of the first n natural frequencies, and the first n modal vectors for the initial state.

$$\boldsymbol{\lambda} = \begin{pmatrix} 60237 & 2682286 & 21391038 & 82438554 & 286161e3 & 748103e3 & 189786e4 & 442507e4 & 152856e6 & 448821e10 \end{pmatrix}$$

State equations are simplified by reducing the initial state to just include the modes of interest, as described in section 3.1. The square root of each eigenvalue is used to calculate the natural frequency in rad/s, and thereafter converted to Hz. f_1 shows first five natural frequencies for the initial system in Hz.

$$\boldsymbol{\lambda} = \begin{pmatrix} 60237 & 2682286 & 21391038 & 82438554 & 286161582 \end{pmatrix}$$

$$\mathbf{U}_1 = \begin{pmatrix} -0.000005 & 0.00011 & 0.00051 & 0.00138 & -0.00340 \\ -0.000001 & 0.000008 & 0.000023 & 0.000046 & -0.000088 \\ -0.184749 & 0.862567 & 1.521322 & 1.535297 & -0.796654 \\ -3.95962 & 13.68743 & 10.37102 & -17.27622 & 68.83187 \\ -0.64779 & 1.52565 & 0.15321 & -1.53923 & 0.260667 \\ -6.37642 & -1.72852 & -3.28287 & -6.21277 & -80.17702 \\ -1.26088 & 0.420824 & -1.25908 & 1.14986 & 0.176068 \\ -7.43893 & -2.20332 & 13.1159 & 21.2392 & 76.3001 \\ -1.92314 & -1.86050 & 1.94283 & -1.87065 & -1.9711 \\ -7.61313 & -27.5937 & 46.6347 & -63.1058 & -96.1961 \end{pmatrix}$$

$$f_1 = \begin{pmatrix} 39 & 261 & 736 & 1445 & 2692 \end{pmatrix}$$

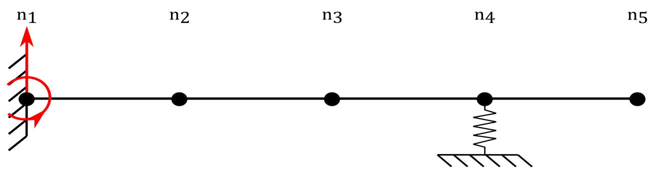

Figure 3: Altered state of the system where the spring is added to the system.

Step 1: Adding roller condition

The inclusion of a roller at node 4 means implementing a boundary condition at DOF 8 according to the specification of an Euler-Bernoulli beam. $\Delta\mathbf{K}_{12}$ depicts the changes in physical space from the initial state to the altered state, where diagonal values shown reflect spring stiffness changes with only the 8th diagonal value as the sole nonzero term with a value of 1e10 N/m. The changes in modal space from the initial to the altered state are represented by $\Delta\overline{\mathbf{K}}_{12}$ which is Eq. 45 in the appendix.

$$\Delta\mathbf{K}_{12} = \begin{pmatrix} 0 & 0 & 0 & 0 & 0 & 0 & 0 & 1e10 & 0 & 0 \end{pmatrix}$$

Downloaded From: https://www.spiedigitallibrary.org/conference-proceedings-of-spie on 19 Apr 2022
Terms of Use: https://www.spiedigitallibrary.org/terms-of-use

Step 2: Spectral decomposition of $\Delta\mathbf{K}_{12}$

The next step is the spectral decomposition of the $\Delta\mathbf{K}_{12}$ matrix using Eq. 15 to obtain the tie and alpha matrix.

$$\mathrm{T} = \begin{pmatrix}1 & 1 & 1 & 1 & 1 & 1 & 1 & 1 & 1 & 1\end{pmatrix}, \qquad \alpha = \begin{pmatrix}0 & 0 & 0 & 0 & 0 & 0 & 0 & 1e10 & 0 & 0\end{pmatrix}$$

Step 3: Set truncation: include only contributing nodes

The contributing vectors are reduced to only those values in the 8th row of each matrix. As a result, Eqs. $\mathbf{U}_{\mathrm{c}}^{\mathrm{T}}$ and $\vec{t}$ can be used to write the contributing modal and tie vectors, resulting in a change vector v as illustrated in Eq. 18.

$$\mathbf{U}_{\mathrm{c}}^{\mathrm{T}} = \begin{pmatrix}-7.4389 & -22.033 & 13.1159 & 21.2392 & 76.3000\end{pmatrix}$$

$$\vec{t} = \begin{pmatrix}0 & 0 & 0 & 0 & 0 & 0 & 0 & 1 & 0 & 0\end{pmatrix}$$

$$\vec{v} = \begin{pmatrix}-7.439 \\ -22.03 \\ 13.12 \\ 21.24 \\ 76.30\end{pmatrix}$$

Step 4: Obtain Ω^2 using Divide and Conquer

With the application of LEMP, the original 10th order GE problem was reduced to a set of 5 second order equations that could be solved using Eq. 27, reducing the complexity of the associated state equation. The squares of the updated natural frequencies are obtained by solving for Ω^2 in Eq. 27.

$$\Omega^2 = \begin{pmatrix}293497 & 0 & 0 & 0 & 0 \\ 0 & 13405181 & 0 & 0 & 0 \\ 0 & 0 & 33185095 & 0 & 0 \\ 0 & 0 & 0 & 101330615 & 0 \\ 0 & 0 & 0 & 0 & 69856604350042\end{pmatrix}$$

Table 3: Ω^2 values using D&C and Sympy function "solveset".

mode	D&C frequency (Hz)	Solveset frequency (Hz)	error (Hz)
1	293496.95719048503	293496.95719048500	58.21 E−12
2	13405184.4772621	13405181.1772621	33.00 E−1
3	33185211.781733	33185095.485877	11.63 E+1
4	101330615.342713	101330615.250119	92.59 E−3
5	69856604350042.539	69856604350042.500	39.06 E−3

Downloaded From: https://www.spiedigitallibrary.org/conference-proceedings-of-spie on 19 Apr 2022
Terms of Use: https://www.spiedigitallibrary.org/terms-of-use

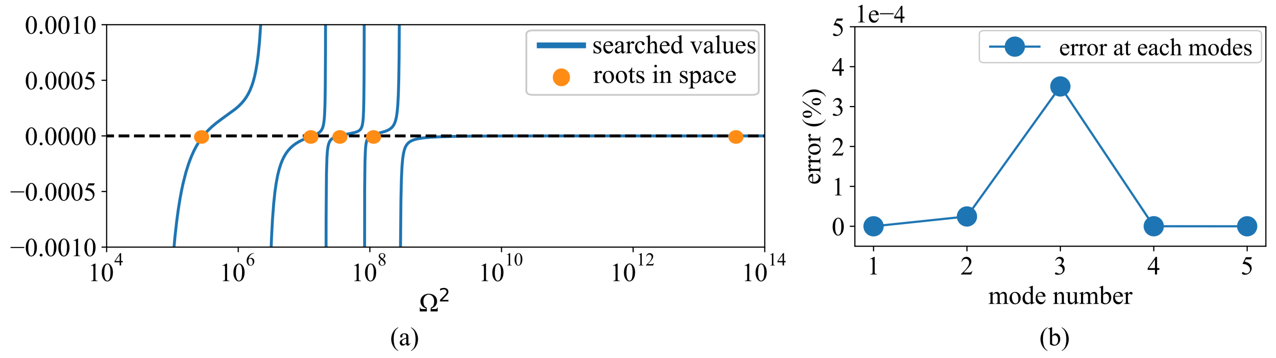

Figure 4: The system's Ω^2 root space showing (a) the five roots of the system, solved for using divide and conquer, and; (b) the error values between the roots found using divide and conquer and Sympy function "solveset".

Figure 4(a) shows the root value for Ω^2 obtained from the root space using the divide and conquer approach; its values are represented at points where the plots pass through zero. The Ω^2 values obtained using divide and conquer are compared to the Sympy function "solveset"[21] as shown in Table 3, similar output is obtained from both methods. Figure 4(b) shows a low percent error between Ω^2 obtained using divide and conquer and the Sympy function "solveset".

Step 5: Solve for new frequencies

The new natural frequencies f_2 in Hz are then calculated for the five modes in the model utilized.

$$f_2 = (86 \quad 583 \quad 917 \quad 1602 \quad 1330221)$$

Step 6: Update roller position

The final step of the process is to use the obtained frequency value to determine the position of the added roller on the beam. This can be done through an error minimization approach, as previously demonstrated by Downey et al.[4]

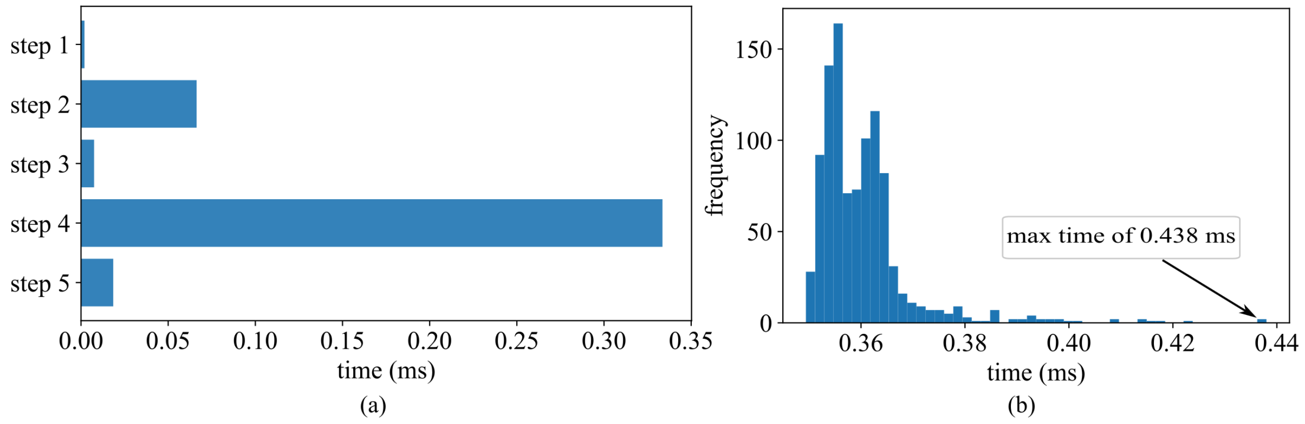

Figure 5: Timing for (a) each step in LEMP algorithm for state estimation, and; (b) the distribution of 1000 simulations of the state estimation process using divide and conquer in the LEMP algorithm.

Figure 5(a) shows the timing of each steps above using the algorithm described in section 3, step 1 takes approximately 0.0019 ms, step 2, 0.0662 ms, step 3, 0.0074 ms, step 4, 0.3353 ms and step 5, 0.0184 ms. A computer with processor Intel(R), Core(TM) i7-10700K CPU 3.80GHz was used for running the test. The total time for a single state estimation using LEMP is approximately 0.4296 ms. Step four in the LEMP process,

Downloaded From: https://www.spiedigitallibrary.org/conference-proceedings-of-spie on 19 Apr 2022
Terms of Use: https://www.spiedigitallibrary.org/terms-of-use

where divide and conquer is used to solve for the altered state frequencies, took the most time at 0.335 ms. This step accounts for approximately 84% of total LEMP time. While the scope of this preliminary work does not contain a full-fledged comparison for the use of the divide and conquer solver against other numerical methods; the divide and conquer solver has proven to be significantly faster than the Sympy "solveset" function which takes about 40 ms to solve the same equation. Figure 5(b) reports a detailed investigation of the timing for step 4. Here, 1000 simulations were performed using the same beam parameters. The min process time is 0.349 ms, while the max is 0.438 ms, and with an average time of 0.361 ms.

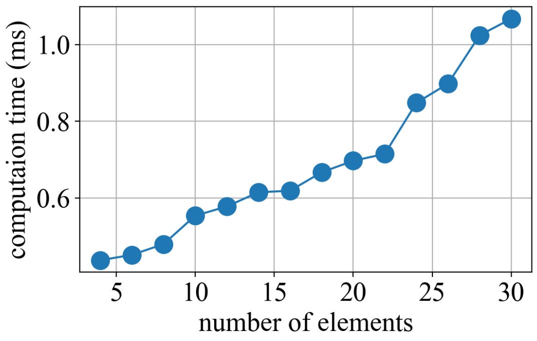

Figure 6: Maximum time required for state estimation using beam with element number 4 to 30.

Figure 6 show the maximum time in 1000 simulations required to achieve single state change estimation using the divide and conquer solver in the LEMP algorithm for different number of elements on the Euler-Bernoulli beam. With a beam of element number 28 and lower, the algorithm easily achieve a state estimation time of less than 1 ms.

4.2 State estimation comparison using LEMP and GE

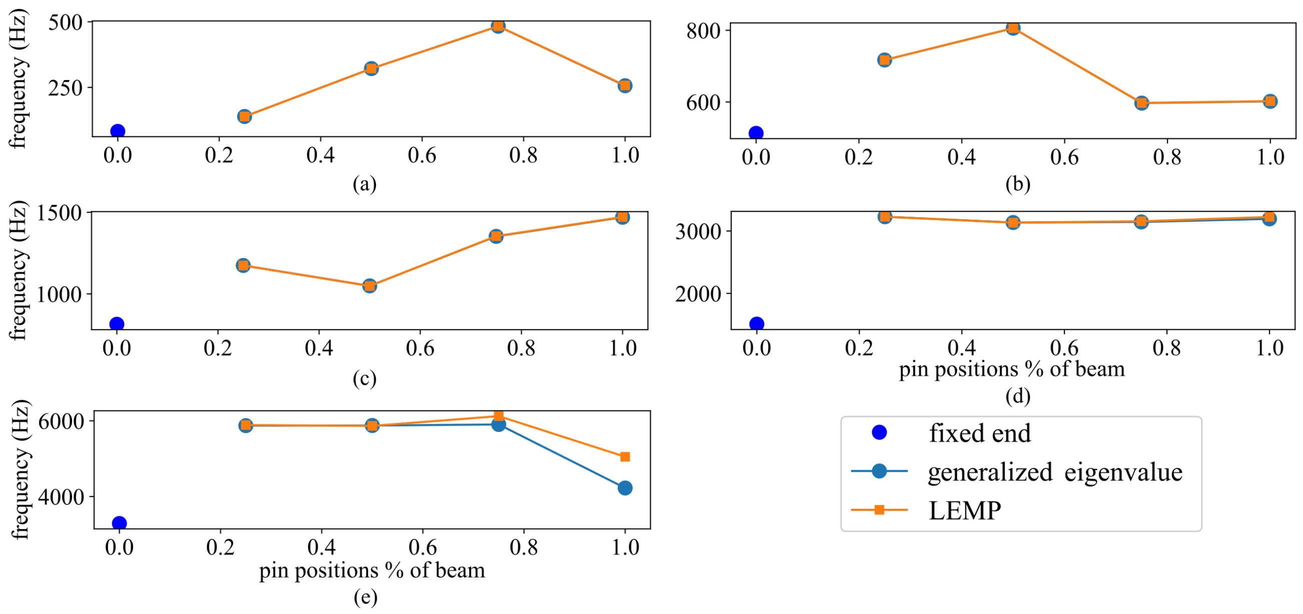

Figure 7: State estimation using LEMP and general eigenvalue for the first five modes of the five node Euler-Bernoulli beam in figure 2.

Downloaded From: https://www.spiedigitallibrary.org/conference-proceedings-of-spie on 19 Apr 2022
Terms of Use: https://www.spiedigitallibrary.org/terms-of-use

With the inclusion of a roller support at node four on the Euler-Bernoulli beam in figure 2, an effective comparison between the LEMP algorithm and the reference GE algorithm is carried out for tracking the system state. Figure 7(a) - (e) shows the state of the beam after the addition of a roller support at node four. A close system state estimation is seen using the Local eigenvalue modification algorithm when compared to the reference general eigenvalue algorithm. Here, the frequencies obtained using the generalized eigenvalue approach is assumed to be the true value, while the LEMP is the estimated frequency value and Eq. 41 and Eq. 42 are used to calculate the error and SNR,. Table 4 show the mean absolute error in Hz and the signal to noise ratio. Small deviations are seen in the fifth mode; however, the percentage error observed is low, and a considerable high SNR is seen in the first four modes as shown in figure 8(a) and (b). This result demonstrates the feasibility of the of the LEMP algorithm with the divide and conqure solver for simple structure. It's viability for more complex state estimations are topic for future works.

Table 4: Mean absolute error and signal to noise ratio for the LEMP and GE.

mode	mean absolute error (Hz)	SNR_{dB}
1	0.2989	30.02
2	0.3193	33.38
3	0.5575	33.54
4	9.8136	25.10
5	262.80	13.18

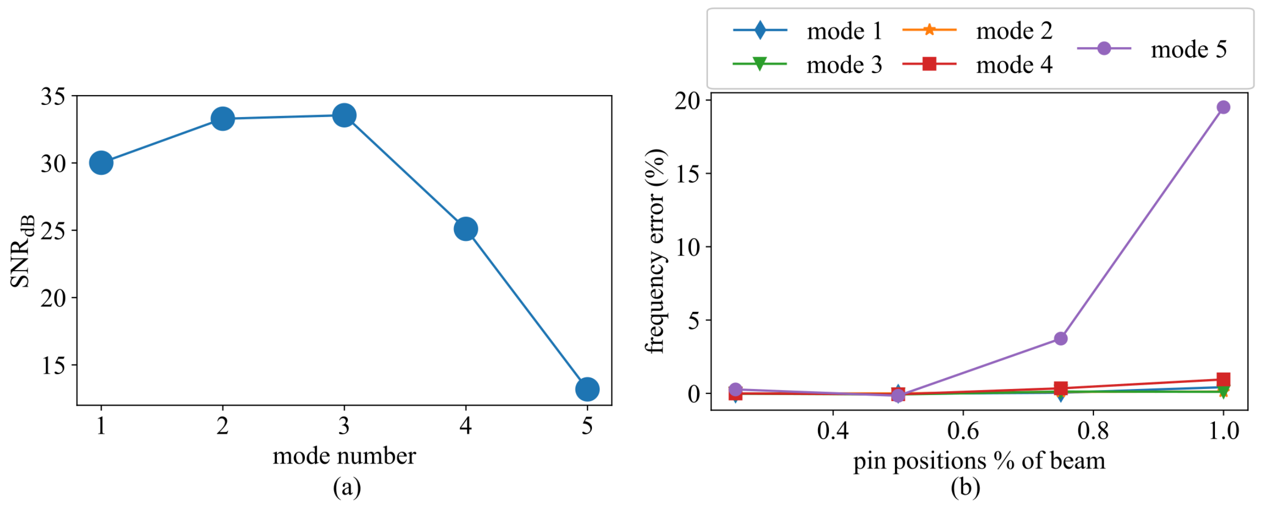

Figure 8: Figure showing the (a) signal to noise ratio for the GE and LEMP state estimation, and; (b) the error in percent between the two approaches.

5. CONCLUSION

The paper demonstrated the potential of using the local eigenvalue modification procedure (LEMP) to estimate the state of a system. The sample five node Euler-Bernoulli beam was used to investigate the timing of each step in the LEMP process for a single-state change. Initial investigation of the LEMP algorithm using the Sympy function "solveset" to solve the resulting secular equation in the LEMP algorithm showed that it took about 40 ms to perform a single-state change update, making it impossible to achieve the the 1 ms time step required for real-time model updating of structures operating in high-rate dynamic environments.

The introduction of the divide and conquer approach to solve the secular equation in the LEMP process formulated a solver that significantly reduced the time taken to solve the system's secular equation. Experimental results demonstrated an average time of 0.361 ms for single state change updating was achieved using the five nodes beam. Using the same 5-nodes beam, an accuracy investigation between the reference general eigenvalue

Downloaded From: https://www.spiedigitallibrary.org/conference-proceedings-of-spie on 19 Apr 2022
Terms of Use: https://www.spiedigitallibrary.org/terms-of-use

algorithm and LEMP with the divide and conquer solver was undertaken. Results showed that the frequencies obtained for state estimation at the nodes from both approaches are close. Signal to noise ratios SNR_{dB} above 20 and low mean absolute error is observed in the first four modes, however, the fifth mode has a lower SNR_{dB} around 14 and higher error. The error at the last node is expected to reduce as the number of nodes in the beam increases. With the addition of the secular equation solver; divide and conquer approach at extremely low latencies, the LEMP algorithm has the potential to enable real-time frequency-based model updating of complex systems that would not be achievable using the general eigenvalue approach.

ACKNOWLEDGMENTS

This material is based upon work supported by the Air Force Office of Scientific Research (AFOSR) through award no. FA9550-21-1-0083. This work is also partly supported by the National Science Foundation Grant numbers 1850012 and 1956071. The support of these agencies is gratefully acknowledged. Any opinions, findings, conclusions, or recommendations expressed in this material are those of the authors, and they do not necessarily reflect the views of the National Science Foundation or the United States Air Force.

REFERENCES

[1] Hong, J., Laflamme, S., Dodson, J., and Joyce, B., "Introduction to state estimation of high-rate system dynamics," *Sensors (Switzerland)* **18** (1 2018).

[2] Dodson, J., Downey, A., Laflamme, S., Todd, M., Moura, A. G., Wang, Y., Mao, Z., Avitabile, P., and Blasch, E., "High-rate structural health monitoring and prognostics: An overview," (2021).

[3] Hong, S. H., Drnek, C., Downey, A., Wang, Y., and Dodson, J., "Real-time model updating algorithm for structures experiencing high-rate dynamic events," (2020).

[4] Downey, A., Hong, J., Dodson, J., Carroll, M., and Scheppegrell, J., "Millisecond model updating for structures experiencing unmodeled high-rate dynamic events," *Mechanical Systems and Signal Processing* **138** (4 2020).

[5] Yang, Z. and Wang, L., "Structural damage detection by changes in natural frequencies," *Journal of Intelligent Material Systems and Structures* **21**, 309–319 (2 2010).

[6] Rainieri, C., Fabbrocino, G., and Cosenza, E., "Near real-time tracking of dynamic properties for standalone structural health monitoring systems," *Mechanical Systems and Signal Processing* **25**, 3010–3026 (11 2011).

[7] Simoen, E., Roeck, G. D., and Lombaert, G., "Dealing with uncertainty in model updating for damage assessment: A review," (5 2015).

[8] Li, W. M. and Hong, J. Z., "New iterative method for model updating based on model reduction," *Mechanical Systems and Signal Processing* **25**, 180–192 (1 2011).

[9] "Effect of local modifications on the vibration characteristics of linear systems 1," (1968).

[10] Drnek, C. R., "Local eigenvalue modification procedure for real-time model updating of structures experiencing high-rate dynamic events," (2020).

[11] Ren-Cang, L., "Solving secular equations stably and efficiently," Tech. Rep. UCB/CSD-94-851, EECS Department, University of California, Berkeley (Dec 1994).

[12] He, J., "Structural modification," *Philosophical Transactions of the Royal Society A: Mathematical, Physical and Engineering Sciences* **359**, 187–204 (2001).

[13] Sestieri, A., "Structural dynamic modification," (2000).

[14] Avitabile, P., "Twenty years of structural dynamic modification – a review," (2021).

[15] Bilbao, S. D., "Numerical sound synthesis, 1st edition," (2009).

[16] Bilbao, S., Desvages, C., Ducceschi, M., Hamilton, B., Harrison-Harsley, R., Torin, A., and Webb, C., "Physical modeling, algorithms, and sound synthesis: The ness project," **43**, 15–30 (2019).

[17] Hallquist, J. and Snyder, V., "Synthesis of two discrete vibratory systems using eigenvalue modification," *AIAA Journal* **11**, 247–249 (1973).

[18] Allemang, R. J., 'te, D. L. B. E., and Soni, M. L., "Experimental modal analysis and dynamic component synthesis vol iv-system modeling techniques d t ic," (1998).

Downloaded From: https://www.spiedigitallibrary.org/conference-proceedings-of-spie on 19 Apr 2022
Terms of Use: https://www.spiedigitallibrary.org/terms-of-use

[19] Zandt, T. V., "Development of efficient reduced models for multi-body dynamics simulations of helicopter wing missile configurations a-ul," (2006).

[20] Avitabile, P. and Pingle, P., "Prediction of full field dynamic strain from limited sets of measured data," *Shock and Vibration* **19**, 765–785 (2012).

[21] Meurer, A., Smith, C. P., Paprocki, M., Čertík, O., Kirpichev, S. B., Rocklin, M., Kumar, A. T., Ivanov, S., Moore, J. K., Singh, S., Rathnayake, T., Vig, S., Granger, B. E., Muller, R. P., Bonazzi, F., Gupta, H., Vats, S., Johansson, F., Pedregosa, F., Curry, M. J., Terrel, A. R., Štěpán Roučka, Saboo, A., Fernando, I., Kulal, S., Cimrman, R., and Scopatz, A., "Sympy: Symbolic computing in python," *PeerJ Computer Science* **2017** (2017).

APPENDIX A.

$$\mathbf{M}_1 = \begin{pmatrix}
0.0828 & 0.0010 & 0.02866 & -0.0006 & 0.0000 & 0.0000 & 0.0000 & 0.0000 & 0.0000 & 0.0000 \\
0.0010 & 0.00002 & 0.0006 & -0.00001 & 0.0000 & 0.0000 & 0.0000 & 0.0000 & 0.0000 & 0.0000 \\
0.0287 & 0.0006 & 0.16564 & 0.0000 & 0.0287 & -0.0006 & 0.0000 & 0.0000 & 0.0000 & 0.0000 \\
-0.0006 & -0.00001 & 0.0000 & 0.00003 & 0.0006 & -0.00001 & 0.0000 & 0.0000 & 0.0000 & 0.0000 \\
0.0000 & 0.0000 & 0.0287 & 0.0006 & 0.1656 & 0.0000 & 0.0287 & -0.0006 & 0.0000 & 0.0000 \\
0.0000 & 0.0000 & -0.0006 & -0.00001 & 0.0000 & 0.00003 & 0.0006 & -0.00001 & 0.0000 & 0.0000 \\
0.0000 & 0.0000 & 0.0000 & 0.0000 & 0.0287 & 0.0006 & 0.1916 & 0.0003 & 0.0377 & -0.0008 \\
0.0000 & 0.0000 & 0.0000 & 0.0000 & -0.0006 & -0.00002 & 0.0004 & 0.00004 & 0.0008 & -0.00002 \\
0.0000 & 0.0000 & 0.0000 & 0.000 & 0.0000 & 0.0000 & 0.0037 & 0.0008 & 0.1088 & -0.0013 \\
0.0000 & 0.0000 & 0.0000 & 0.0000 & 0.0000 & 0.0000 & -0.0008 & -0.00001 & -0.0013 & 0.00002
\end{pmatrix} \tag{43}$$

$$\mathbf{K}_1 = \begin{pmatrix}
10000000000 & 177960 & -4067661 & 177960 & 0.00000 & 0.0000 & 0.0000 & 0.0000 & 0.0000 & 0.0000 \\
177960 & 10000000000 & -177960 & 5191 & 0.0000 & 0.0000 & 0.0000 & 0.0000 & 0.0000 & 0.0000 \\
-4067661 & -177960 & 8135322 & 0.0000 & -40676616 & 177960 & 0.0000 & 0.0000 & 0.0000 & 0.0000 \\
177960 & 5191 & 0.0000 & 20762 & -177960 & 5191 & 0.000 & 0.0000 & 0.000 & 0.0000 \\
0.0000 & 0.0000 & -4067661 & -177960 & 8135322 & 0.0000 & 4067661 & 177960 & 0.0000 & 0.0000 \\
0.0000 & 0.0000 & 177960 & 5191 & 0.0000 & 20762 & -177960 & 5191 & 0.0000 & 0.0000 \\
0.0000 & 0.0000 & 0.0000 & 0.00000 & -4067661 & -177960 & 8135322 & 0.0000 & -4067661 & 1779601 \\
0.00000 & 0.00000 & 0.0000 & 0.0000 & 177960 & 5191 & 0.0000 & 20762 & -177960 & 5191 \\
0.0000 & 0.0000 & 0.0000 & 0.0000 & 0.0000 & 00000 & -4067661 & -177960 & 4067661 & -177960 \\
0.0000 & 000000 & 000000 & 000000 & 000000 & 000000 & 177960 & 5191 & -177960 & 10381
\end{pmatrix} \tag{44}$$

$$\Delta\overline{\mathbf{K}}_{12} = \begin{pmatrix}
-0.000005 & -0.000001 & -0.184749 & -3.95962 & -0.64779 & -6.37642 & -1.26088 & -7.43893 & -1.92314 & -7.61313 \\
0.00011 & 0.000008 & 0.862567 & 13.68743 & 1.52565 & -1.72852 & 0.420824 & -2.20332 & -1.86050 & -27.5937 \\
0.00051 & 0.000023 & 1.521322 & 10.37102 & 0.15321 & -3.28287 & -1.25908 & 13.1159 & 1.94283 & 46.6347 \\
0.00138 & 0.000046 & 1.535297 & -17.27622 & -1.53923 & -6.21277 & 1.14986 & 21.2392 & -1.87065 & -63.1058 \\
-0.00340 & -0.000088 & -0.796654 & 68.83187 & 0.260667 & -80.17702 & 0.176068 & 76.3001 & -1.9711 & -96.1961 \\
0.00733 & 0.00016 & -0.14115 & -121.432 & 1.41143 & 31.5312 & -0.90337 & 95.7498 & -2.13004 & -145.1654 \\
0.013243 & 0.000275 & -0.85067 & -136.014 & 0.41132 & -177.991 & 1.1859 & -26.0798 & 2.36921 & 2.21619 \\
-0.00839 & -0.000166 & 0.383631 & 45.9726 & 0.47523 & 119.004 & 0.52428 & 208.532 & 4.36167 & 510.2967 \\
-3.90516 & -0.039731 & 0.54904 & -86.337121 & 0.18177 & -26.36656 & 0.048352 & -8.26030 & -0.049201 & -7.5236 \\
6.84523 & -669.907 & 1.06031 & -144.603 & 0.28573 & -40.5525 & 0.074222 & -12.3722 & -0.07115 & -10.9945
\end{pmatrix} \tag{45}$$

Downloaded From: https://www.spiedigitallibrary.org/conference-proceedings-of-spie on 19 Apr 2022
Terms of Use: https://www.spiedigitallibrary.org/terms-of-use